Cancer Cell
Article

URI Is an Oncogene Amplified in Ovarian Cancer Cells and Is Required for Their Survival

Jean-Philippe Theurillat,[1,2,4] Stefan Christian Metzler,[1,4] Nico Henzi,[2] Nabil Djouder,[1] Marianne Helbling,[1] Anna-Kathrin Zimmermann,[2] Francis Jacob,[3] Alex Soltermann,[2] Rosmarie Caduff,[2] Viola Heinzelmann-Schwarz,[3] Holger Moch,[2,4,*] and Wilhelm Krek[1,4,*]
[1]Institute of Cell Biology, ETH Zurich, 8093 Zurich, Switzerland
[2]Institute of Surgical Pathology, Department Pathology
[3]Department Gynecology and Obstetrics
University Hospital Zurich, 8091 Zurich, Switzerland
[4]These authors contributed equally to this work
*Correspondence: holger.moch@usz.ch (H.M.), wilhelm.krek@cell.biol.ethz.ch (W.K.)
DOI 10.1016/j.ccr.2011.01.019

SUMMARY

Abrogation of negative feedback control represents a fundamental requirement for aberrantly activated signaling pathways to promote malignant transformation and resistance to therapy. Here we identify *URI*, which encodes a mitochondrial inhibitor of PP1γ and PP1γ-mediated feedback inhibition of S6K1-BAD survival signaling, as an oncogene amplified and overexpressed in ovarian cancer cell lines and human ovarian carcinomas. *URI* is an "addicting" oncogene selectively required for the survival of ovarian cancer cells with increased *URI* copy number. By constitutively detaining PP1γ in inactive complexes, URI sustains S6K1 survival signaling under growth factor–limiting conditions and mediates resistance of cells to cisplatin. Thus, oncogenic activation of *URI* defines an important mechanism for activating mitochondrial S6K1-BAD signaling and promoting cell survival through disabling PP1γ-dependent negative feedback inhibition.

INTRODUCTION

Tumorigenesis is a multistep process, in which mutations in key cellular genes produce a series of acquired capabilities that allow the developing cancer cell to survive many stresses, including limitations of oxygen, glucose, growth factors, and nutrients (Johnstone et al., 2002). Because many of these stresses activate the intrinsic apoptotic pathway at mitochondria, the ability of cancer cells to evade this death pathway has become an established hallmark of cancer (Hanahan and Weinberg, 2000). The fact that this mitochondrial apoptotic pathway operates under conditions of physiological and drug-induced cell death explains also why the very genetic alterations that mediate intrinsic resistance to physiologic death stimuli also lead to inherent resistance of cancer cells to numerous chemotherapeutic drugs (Johnstone et al., 2002).

Genetic alterations affecting life-death decisions at mitochondria often deregulate intracellular signaling pathways that transduce survival signals. Prominent among these are the phosphatidylinositol 3-kinase (PI3K)–Akt/PKB and the mammalian target of rapamycin (mTOR)–S6K1 pathways that modulate the activity of members of the Bcl-2 family of pro- and antiapoptotic proteins (Bergmann, 2002). Both Akt/PKB and S6K1 have been shown to phosphorylate, as part of their prosurvival functions, the proapoptotic BH3-only protein BAD at distinct sites, which in turn sequesters BAD in the cytoplasm, thereby preventing

Significance

Augmentation of signaling output and elicitation of cancer phenotypes by activated signaling pathways depends on abrogation of negative feedback mechanisms by oncogenic events that directly target components of the feedback system. Such oncogenic events and the signaling pathways they affect are expected to constitute targets for "targeted" therapies with reduced nonspecific drug-associated toxicity. We describe here the discovery of an ovarian cancer oncogene, *URI*, whose gene product abrogates negative feedback on S6K1 survival signaling, thereby enhancing cell survival. Abrogation of this feedback renders *URI*-amplified ovarian cancer cells also resistant to cisplatin-induced apoptosis. These findings have implications for the development of mechanism-based therapies targeting the URI cancer pathway in patients whose tumors are characterized by *URI* amplification.

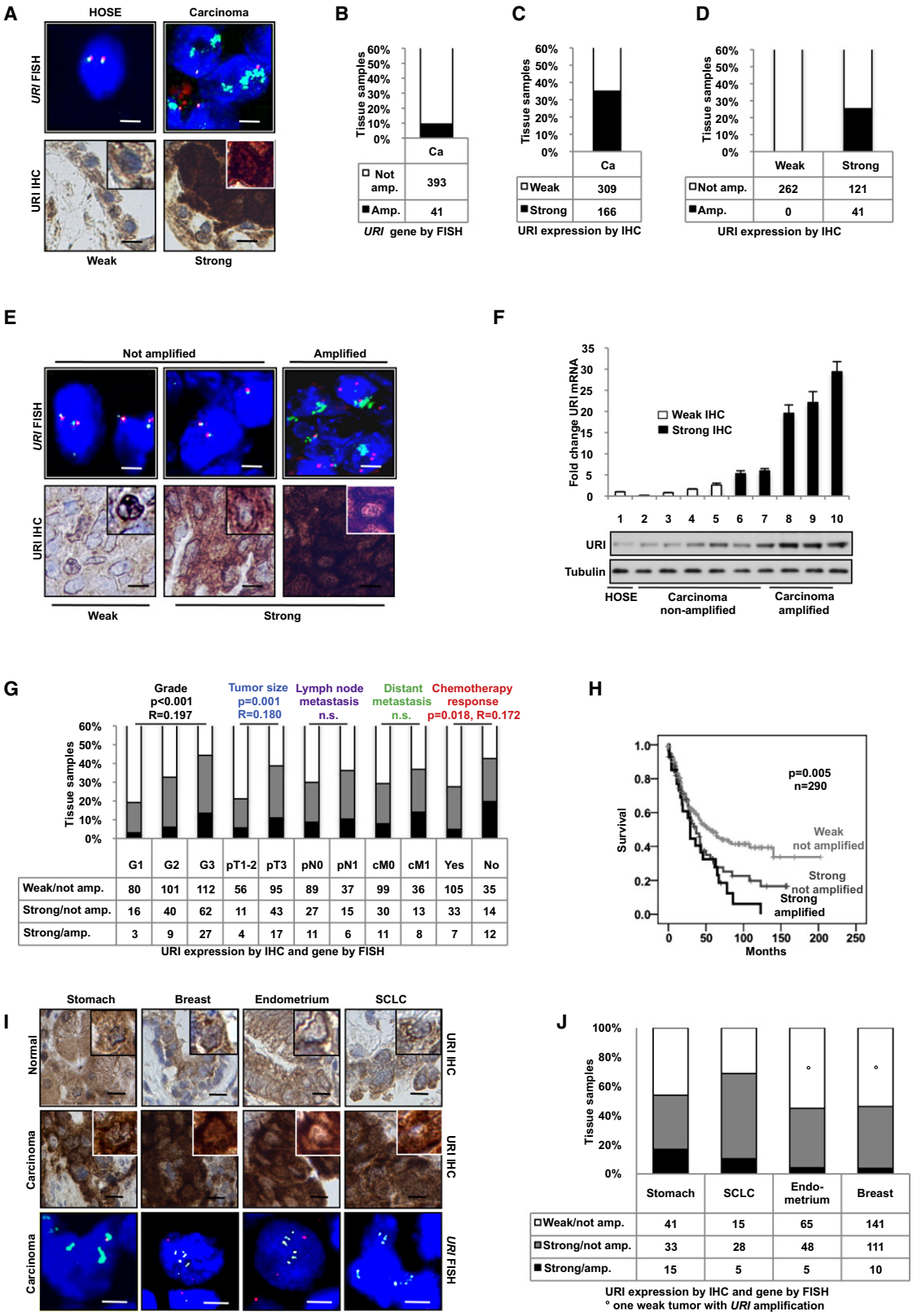

Figure 1. *URI* Amplification Correlates with Aggressive Behavior in Ovarian Cancer

(A) Ovarian cancers analyzed by fluorescence in situ hybridization (FISH) analysis with green and red probes detecting *URI* and the chromosome 19 centromer, respectively, and by immunohistochemistry (IHC) for URI protein using TMAs. Diploid human ovarian surface epithelium (HOSE) and carcinomas (Ca) with normal

association of BAD with Bcl-2 or Bcl-X_L proteins (Bergmann, 2002; Datta et al., 2002; Harada et al., 2001). This mechanism enhances resistance of cells to undergo apoptosis in response to death cues (Bergmann, 2002; Datta et al., 2002; Harada et al., 2001). It also links growth factor and nutrient signals integrated via the PI3K-Akt/PKB and mTOR-S6K1 pathways to the regulation of cell survival. Counterbalancing the activity of survival kinase-mediated phosphorylation of BAD are phosphatases, including mitochondria-associated phosphatase 1 gamma (PP1γ) (Danial et al., 2003; Djouder et al., 2007; Klumpp and Krieglstein, 2002). It has been demonstrated that the ability of PP1γ to function as a phosphatase counterbalancing S6K1-BAD survival signaling depends, in part, on the phosphorylation status of its interaction partner URI, a member of the prefoldin family of molecular chaperones (Gstaiger et al., 2003; Siegert et al., 2000). In its un(der)phosphorylated form, URI is bound to PP1γ and functions as its inhibitor. Dissociation of PP1γ from bound URI is initiated by S6K1-mediated phosphorylation of URI at Ser-371, which when liberated, proceeds to dephosphorylate S6K1 and possibly BAD (Djouder et al., 2007). On the basis of these findings, a model has been proposed in which acute activation of S6K1 in response to growth factor and nutritional cues triggers a negative feedback system operating at mitochondria that involves the phosphorylation of URI and the subsequent liberation of PP1γ, which dampens S6K1 survival signaling. Under growth factor and nutrient-rich conditions, this negative feedback system operates at basal/low levels.

On the basis of the above-noted model, it follows that during tumor evolution, genetic alterations abrogating the normal operation of this negative feedback system could result in enhanced signaling output (i.e., increased S6K1 cell survival) and consequently increased resistance of cells to apoptosis in response to stress cues. In this context, the chromosomal locus 19q12 where *URI* resides was found amplified in a variety of carcinomas (Leung et al., 2006; Lin et al., 2000; Nakanishi et al., 2000; Schraml et al., 2003; Snijders et al., 2003). Moreover, the 19q12 amplicon has been shown in a genomewide screen to correlate with resistance against platinum-based chemotherapy in ovarian cancer (Etemadmoghadam et al., 2009). Despite attempts to improve therapeutic options for this cancer type, malignancies derived form the normal surface epithelium have still the worst prognosis among gynecological tumors and since decades, standard treatment consists of platinum-based chemotherapy after surgery.

Given these observations, we tested in this study the hypothesis that oncogenic activation of *URI* occurs in a subset of ovarian cancers and contributes in this setting to increased ovarian cancer cell survival by disabling negative feedback control on S6K1 signaling. We also investigated whether the gene product of *URI* might contribute to resistance of ovarian cancer cells to cisplatin and rapamycin.

RESULTS

URI Amplification Correlate with Aggressive Behavior in Ovarian Cancer

A number of studies reported copy number gain or amplification of 19q12 in ovarian cancer (Etemadmoghadam et al., 2009; Hu et al., 2003; Lin et al., 2000; Schraml et al., 2003). Because the *URI* locus resides within this amplified region, we analyzed *URI* gene copy alterations by fluorescence in situ hybridization (FISH) and protein expression by immunohistochemical staining (IHC) of human ovarian cancer specimens derived from two different cohorts (Figure 1; see Figure S1A available online).

URI amplification, as defined by the presence of at least six gene copies per nucleus, was detectable in ~10% of ovarian carcinomas, with no preference for histological subtype (Figures 1A and 1B; Figure S1B). The majority of cases (36 of 41 ovarian tumors) harbored more than 10 copies of the *URI* locus per nucleus (data not shown). *URI* amplification was detectable in neither normal human ovarian surface epithelium (HOSE) (Figure 1A) nor other types of ovarian malignancies, such as noninvasive borderline or ovarian germ cell tumors (data not shown).

Next we determined whether ovarian carcinomas are characterized by increased URI protein levels. URI expression was assessed by IHC of human ovarian cancer specimens on tissue microarrays, and the average of the individual scores of a two-tiered scoring system (weak versus strong) evaluated by three different pathologists was used for subsequent analysis. As shown in Figure S1C, the interobserver variability was low. The URI antibody used in this study specifically detects endogenous URI on paraffin-embedded sections (Figure S1D). In almost 40% of cases, we detected high levels of URI (Figure 1C), compared to HOSE, where expression of URI was defined as weak (Figure 1A). By complementing this data set with *URI* gene copy alterations, we found that all ovarian cancers with *URI* amplification consistently displayed URI overexpression and that a subset of ovarian cancers without *URI* amplification still expressed high levels of URI (Figures 1D and 1E). These results imply that *URI* gene copy alterations represent one mechanism of deregulation of URI protein expression. Consistent with this notion, we observed the highest levels of URI mRNA and protein levels in

(weak) URI expression and high-copy amplified carcinomas with overexpression (strong) are shown. Bars represent 5 μm (FISH) and 12 μm (IHC). Inlays with higher magnification highlight expression levels within one cell using adjusted contrast/brightness settings for each individual cell (see also below).
(B and C) *URI* amplification and URI protein expression.
(D and E) Correlation between *URI* amplification and protein expression. Bars represent 5 μm (FISH) and 12 μm (IHC).
(F) Fold change mRNA expression normalized to human primary HOSE by quantitative RT-PCR and corresponding protein expression by western blot of selected cases.
(G) Correlation of URI protein expression/amplification with clinicopathological parameters (R = correlation coefficient; p = Kendall beta-tau). Expression was stratified into three groups: (i) weak protein expression/*URI* not amplified, (ii) strong expression/not amplified, and (iii) strong expression/*URI* amplified.
(H) Corresponding Kaplan-Meier survival analysis (p = Log rank).
(I and J) *URI* FISH and IHC of normal epithelium and adenocarcinomas of the stomach, endometrium, breast, and small-cell lung cancer (SCLC) on TMA. Bars represent 5 μm (FISH) and 10 μm (IHC). Differences in number of cases among immunohistochemical markers were due to tissue damage (either tissue loss or inadequate tumor tissue), a problem associated with TMAs.
See also Figure S1.

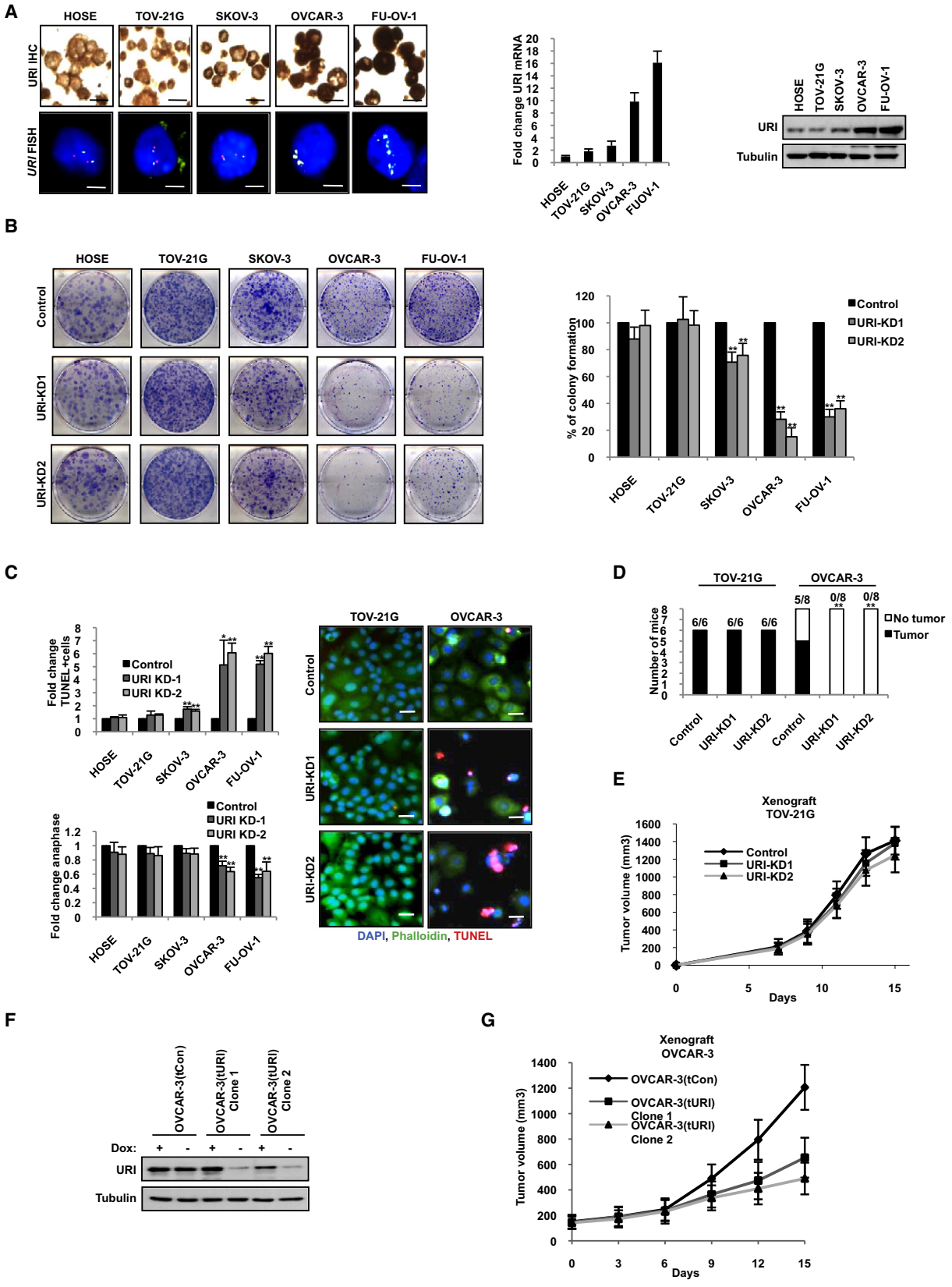
A
HOSE
TOV-21G
SKOV-3
OVCAR-3
FU-OV-1
URI IHC
URI FISH
Fold change URI mRNA
HOSE
TOV-21G
SKOV-3
OVCAR-3
FUOV-1
URI
Tubulin
B
Control
URI-KD1
URI-KD2
% of colony formation
C
Fold change TUNEL+cells
Control
URI KD-1
URI KD-2
Fold change anaphase
TOV-21G
OVCAR-3
DAPI, Phalloidin, TUNEL
D
Number of mice
6/6
5/8
0/8
No tumor
Tumor
E
Xenograft TOV-21G
Tumor volume (mm3)
Days
F
OVCAR-3(tCon)
OVCAR-3(tURI) Clone 1
OVCAR-3(tURI) Clone 2
Dox:
URI
Tubulin
G
Xenograft OVCAR-3

those ovarian cancers characterized by *URI* gene copy alterations (Figure 1F).

To assess whether *URI* amplification and/or overexpression is associated with clinicopathological parameters of tumor aggressiveness, we subdivided ovarian carcinomas into three groups according to *URI* amplification/protein expression patterns: (1) weak expression and not amplified, (2) strong expression and not amplified, and (3) strong expression and amplified. Importantly, the latter group was characterized by higher histological grade, broader tumor spread (pT), and failure to respond to platinum-based chemotherapy (Figure 1G). In contrast, the moderate URI protein expression seen in the absence of *URI* amplification was linked to broader tumor spread but not to grade or chemotherapy response (Figure 1G), implying that either the higher protein expression of URI in the context of amplification or other coamplified genes at 19q12 may contribute to a more malignant phenotype. We did not observe significant correlations with lymphatic (pN) or distant metastatic spread (cM) in any of the above-noted three groups (Figure 1G).

URI amplification and protein expression correlated significantly with poor disease-specific patient's survival (Figure 1H). Similar observations were obtained when the two different ovarian cancer cohorts were analyzed separately or when the pooled cohorts were evaluated by three different observers (Figures S1E and S1F). The quality of survival data sets used in this study are illustrated by Kaplan-Meier curves of established prognostic factors including tumor spread (pT) and chemotherapy response (Figure S1G).

Amplification at 19q12 has been described in other carcinoma entities (Leung et al., 2006; Lin et al., 2000; Schraml et al., 2003; Snijders et al., 2003). Interestingly, we found a substantial number of cancers characterized by *URI* amplification and overexpression, including adenocarcinomas of the stomach, endometrium, breast (with medullary histology), and small-cell lung cancer (SCLC) (Figures 1I and 1J). Thus, *URI* is amplified and overexpressed in a substantial fraction of several distinct cancer types.

Consequences of Suppression of URI Function in Ovarian Cancer Cells

Many oncogenes, when overexpressed, render cancer cells dependent on the continued function of the oncogene for cell proliferation or survival. Because the above-noted data imply that *URI* may function as an oncogene, we tested whether ovarian cancer cells are functionally dependent on URI. To this end, we selected a panel of five cell lines of ovarian origin that reflected best the different URI levels encountered in human tissue. Immortalized HOSE cells express low levels of URI mRNAs and protein (Figure 2A). Human ovarian surface carcinoma TOV-21G and SKOV-3 cells, which do not display *URI* gene copy alterations, express low to moderate levels of URI mRNAs and protein, whereas human ovarian surface carcinoma OVCAR-3 and FU-OV-1 cells are both characterized by *URI* amplification and high levels of URI mRNA and protein expression (Figure 2A).

Using two different short-hairpin RNAs (shRNAs) targeting URI mRNAs, we assessed the effects of URI depletion on colony formation of these different ovarian cell lines. Immunoblotting confirmed that URI depletion was very efficient (Figure S2A). Strikingly, URI depletion selectively reduced colony formation of OVCAR-3 and FU-OV-1 cells (Figure 2B). This effect was considerably less pronounced or absent in SKOV-3 or TOV-21G cells, respectively (Figure 2B). Consistent with this finding, URI knockdown caused significant cell death of OVCAR-3 and FU-OV-1 cells but not of SKOV-3, TOV-21G, or HOSE cells, as evidenced by TUNEL staining (Figure 2C). In accordance with this finding, the number of detectable anaphase cells, assessed in parallel as an indicator of active proliferation, was selectively reduced in URI-depleted OVCAR-3 and FU-OV-1 cells (Figure 2C). In addition, URI depletion caused also cell death in cancer cell lines of nonovarian origin that are characterized by *URI* amplification including MKN-7 (gastric cancer), Lu-143 (SCLC), EFE-184 (endometrial cancer), and MDA-MB-157 (medullary breast cancer) (Figures S2B and S2C). Finally, URI knockdown in *URI*-amplified OVCAR-3 cells abolished their ability to form tumors in immunodeficient mice (Figure 2D). In contrast, there was no negative effect on tumor growth or on the kinetics of tumor growth when URI was depleted from TOV-21G cells (Figure 2E). In each case, URI depletion was effective, as evidenced by immunoblotting analysis (data not shown).

To assess a potential requirement of URI for tumor growth after tumor establishment, we established OVCAR-3 cell lines expressing tetracycline (tet)–regulable (tet-off) microRNA-based hairpins (Dickins et al., 2005) targeting URI mRNAs, referred to as OVCAR-3(tURI), or a "scrambled" control shRNA, referred to as OVCAR-3(tCon). In the presence of doxycycline, OVCAR-3 (tCon) and OVCAR-3(tURI) cell lines expressed similar levels of

Figure 2. Consequences of Suppression of URI Function in Ovarian Cancer Cells

(A) Immunohistochemical, FISH, quantitative RT-PCR, and immunoblot analysis of ovarian cell lines without (HOSE, TOV-21G, SKOV-3) and with *URI* amplification (OVCAR-3, FU-OV-1). Bars represent 15 μm (IHC) and 5 μm (FISH).

(B) Clonogenic assay and quantification of ovarian cell lines after URI knockdown with two different short hairpin RNAs (KD1, KD2; immunoblot knockdown validation) (see Figure S2A) of three independent experiments in triplicate (*$p < 0.05$ and **$p < 0.01$, Student's t test).

(C) TUNEL staining with quantification and analysis of anaphases after URI depletion of three independent experiments in triplicate (*$p < 0.05$ and **$p < 0.01$, Student's t test). Bars represent 15 μm.

(D) Number of tumors grown subcutaneously in nude mice after injection of TOV-21G or OVCAR-3 cells (**< 0.01, Student's t test).

(E) Tumor size increase over time of control and URI knockdown TOV-21G cells in xenograft experiments using 6 mice per group.

(F) Immunoblotting of whole cell extracts derived from two different clones of OVCAR-3(tURI) or OVCAR-3(tCon) cells in the presence or absence of doxycyline for indicated proteins.

(G) Tumor growth of two different clones of OVCAR-3(tURI) or OVCAR-3(tCon) in a xenograft mouse model. Doxycycline was removed from the drinking water 5 days after injection of the indicated cells. Xenograft experiments represent 6 mice for OVCAR-3(tURI) (Clone 1) and 7 mice for each OVCAR-3(tURI) (Clone 2) and OVCAR-3(tCon). Time point 0 indicates the start of the volume measurements.

All error bars in the entire figure represent ± SD. See also Figure S2.

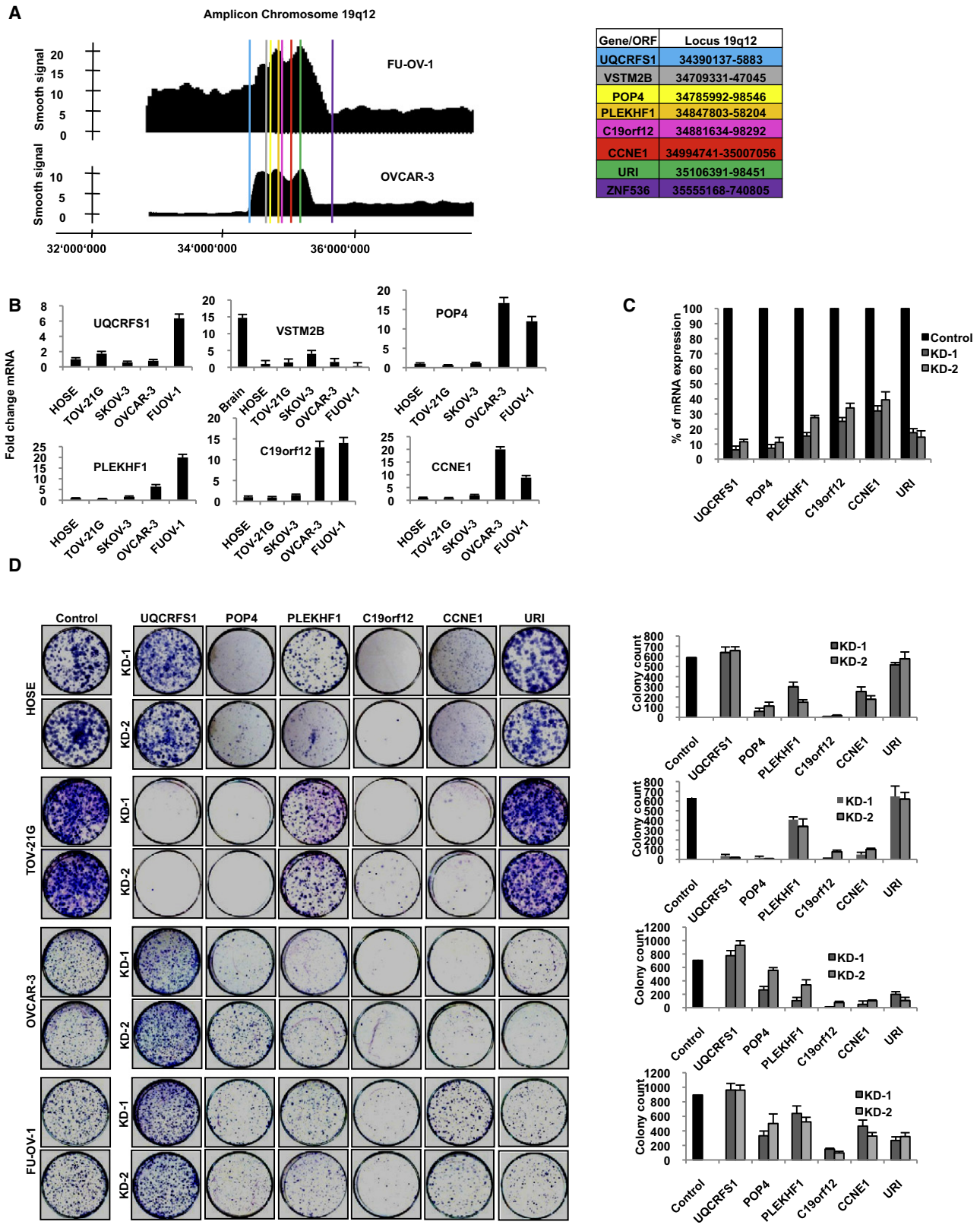

Figure 3. Requirements of 19q12 Coamplified Genes for Cell Survival of Ovarian Cancer Cells

(A) Quantitative SNP array analysis of the 19q12 amplicon of FU-OV-1 and OVCAR-3 cells. All known coding genes within this region are highlighted by different colors.

URI. However, removal of doxycycline induced efficient reduction of URI selectively in the OVCAR-3(tURI) cell lines (Figure 2F). Consistent with this result, the ability of OVCAR-3(tURI) cell lines to form colonies also was substantially reduced in the absence of doxycycline (Figure S2D). Given these cell-culture data, we next injected OVCAR-3(tCon) and OVCAR-3(tURI) cell lines subcutaneously into the flanks of nude mice treated with doxycycline. Importantly, removal of doxycycline after limited tumor growth in vivo reduced further tumor progression of the OVCAR-3 (tURI) xenografts but not of the OVCAR-3(tCon) xenografts (Figure 2G). These results suggest that URI function is required both for de novo tumorigenesis and for further tumor progression after tumor establishment.

Requirements of 19q12 Coamplified Genes for Cell Survival of Ovarian Cancer Cells

Next we asked whether these ovarian cancer cells are similarly dependent for their survival on other genes coamplified at 19q12. SNP array analysis of FU-OV-1 and OVCAR-3 cells revealed a circumscribed amplicon at 19q12 encompassing seven genes (in FU-OV-1 cells) and six genes (in OVCAR-3 cells) (Figure 3A). In both cell lines, *URI* located precisely at the last peak of the amplicon, in FU-OV-1 cells even being the most amplified gene in the entire genome (data not shown). In fact, a comparative analysis of gene amplification at 19q12 between 116 human ovarian carcinomas (Etemadmoghadam et al., 2009) and FU-OV-1 and OVCAR-3 cells revealed a similar pattern of coamplified genes (Figures S3A and S3B).

All genes present in the amplicon were up-regulated in ovarian cancer cells harboring an amplification, except *VSTM2B*, encoding V-set and a transmembrane domain containing 2B, which was expressed at very low levels in all cell lines tested (Figure 3B). To assess the functional significance of these genes with respect to cell survival in the context of 19q12 amplification, we performed clonogenic assays in nonamplified (HOSE, TOV-21G) and amplified (OVCAR-3, FU-OV-1) ovarian cells by depleting individually the mRNAs derived from all coding genes at 19q12 (except for *VSTM2B*) using two different shRNAs (Figure 3C). Strikingly, depletion of POP4, encoding processing of precursor 4, PLEKHF1, encoding pleckstrin homology domain containing, family F (with FYVE domain) member, C19orf12, encoding chromosome 19 open reading frame 12, and CCNE1, encoding cyclin E, drastically reduced colony count in all cell lines analyzed, indicating that within the core of the amplicon, four genes were found to be essential for cell proliferation independent of 19q12 amplification status (Figure 3D). Depletion of UQCRFS1, encoding ubiquinol-cytochrome C reductase Rieske iron-sulfur polypeptide, enhanced colony formation in all cell lines except of TOV-21G (Figure 3D). This analysis indicates that *URI* is the only coding gene within the amplicon 19q12 whose depletion selectively affects colony formation of cells with a 19q12-amplification.

URI Sustains Survival of *URI*-Amplified Ovarian Cancer Cells Through a PP1γ-Dependent Mechanism

Recently we reported that URI binds to and inhibits PP1γ, an interaction dynamically regulated by S6K1-mediated phosphorylation of URI at Ser-371 (Djouder et al., 2007). Because URI is highly overexpressed in ovarian cancer cells, in particular in those with a 19q12 amplicon, and is required in these cells for cell survival, we asked whether part of its potential oncogenic function derives from its capacity to maintain PP1γ constitutively bound to it. Consequently, PP1γ would be inhibited and its proapoptotic function abolished. As shown in Figure 4A, the amount of URI coimmunoprecipitating with PP1γ from different ovarian cell lines correlated with the degree of URI overexpression (Figures 2A and 4A). We note that unlike URI, PP1γ expression does not vary significantly in these cell lines (Figure 4A). Similar results were obtained in human tissues, where the highest amount of URI-PP1γ complexes was detected in those carcinomas with *URI* amplification (Figure S4A). Phosphorylation of URI at Ser-371 is known to mediate disruption of URI-PP1γ complexes. Because ovarian cancer cell lines overproducing URI are characterized by increased abundance of URI-PP1γ complexes, one might predict that in these cells phosphorylation of URI at Ser-371 is low. Indeed, we observed little variation in Ser-371 phosphorylation of URI among the different cell lines (Figure 4B), implying that up-regulation of URI protein and Ser-371 phosphorylation is uncoupled.

According to the above-noted hypothesis, cell death induced by URI depletion should be dependent on PP1γ function. As shown in Figure 4C, decreases in cell number and the number of anaphases as well as the increase in apoptosis associated with URI depletion in FU-OV-1 cells is rescued by concomitant knockdown of PP1γ. Immunoblotting revealed that S6K1 and its downstream target BAD were dephosphorylated at Thr-389 and Ser- 136, respectively, in URI-depleted cells (Figure 4D). Combined knockdown of URI and PP1γ recovered the phosphorylation of both S6K1 and BAD at these sites. These results are in line with the view that URI has properties of an oncoprotein in ovarian cancer cells with a 19q12 amplicon and that it functions, in part, by detaining PP1γ inactive and disabling the negative feedback to limit S6K1 survival signaling.

To further corroborate this hypothesis, we tested next whether overexpression of URI might promote resistance against apoptosis in otherwise not-amplified TOV-21G cells that naturally display low URI levels. To this end, we generated retrovirally infected TOV-21G cell pools stably expressing HA-tagged URI (wt) or URI(S371A) phosphosite mutant, which constitutively entraps PP1γ and thus is expected to closely mimic the potential oncogenic properties of URI. Both HA-tagged URI species are produced to similar levels in these pools, and the degree of overexpression of these HA-tagged URI species is moderate (2–3 fold over endogenous URI) (Figure S4C). Importantly, we found significantly more HA-URI(S371A) protein coimmunoprecipitating with

(B) mRNA expression by quantitative RT-PCR (qPCR) of amplified genes in cell lines as indicated. Silenced VSTM2B expression (cycle threshold >36 for all cell lines, brain represents positive control).

(C) Characterization of knockdown efficiency in FU-OV-1 cells with two different short hairpin RNAs used against indicated genes by qPCR.

(D) Clonogenic assay and quantification of indicated cell lines after knockdown of the genes identified to be amplified at 19q12 of three independent experiments in triplicate.

All error bars represent ± SD in the entire figure. See also Figure S3.

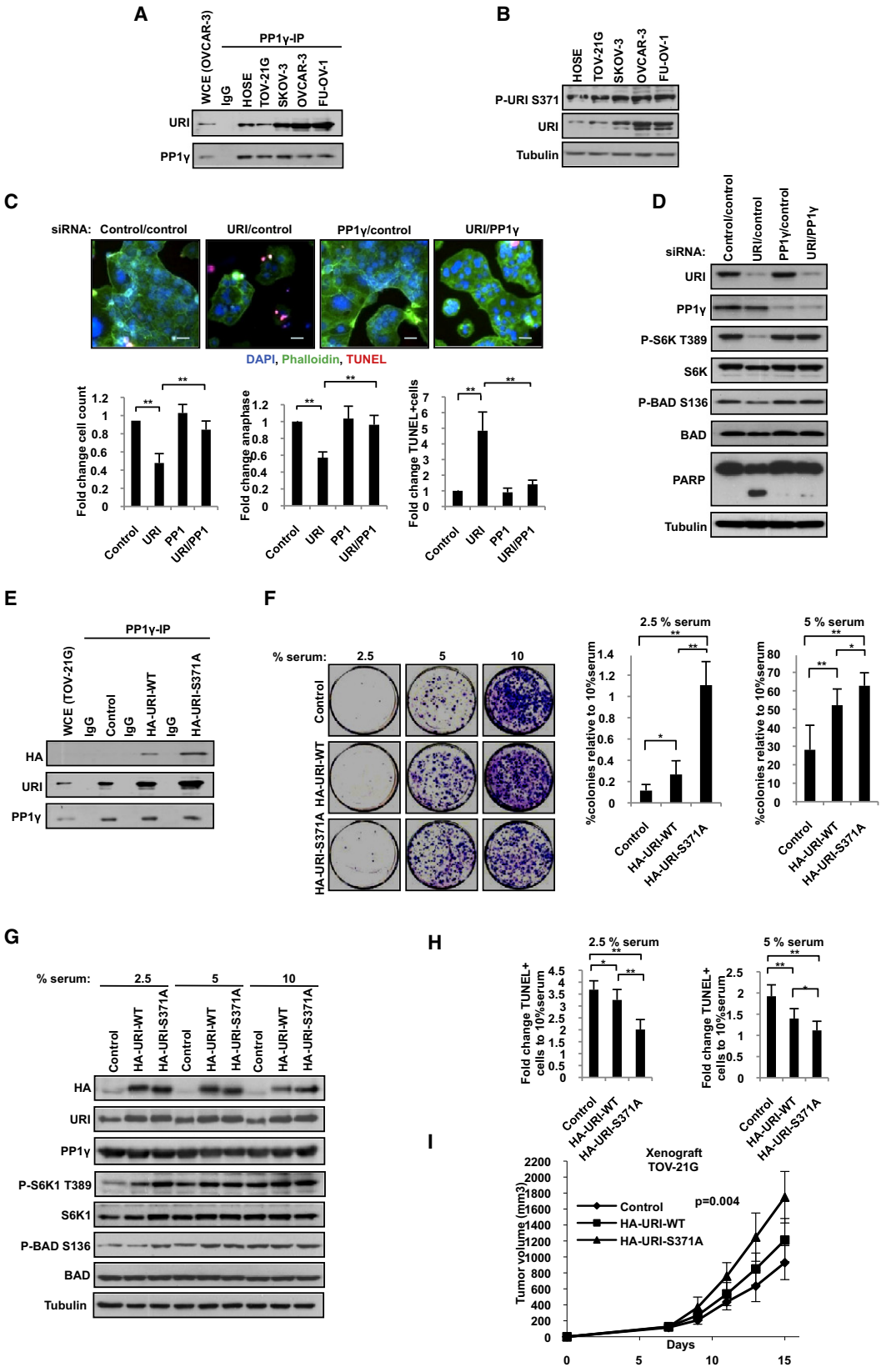
A
PP1γ-IP
WCE (OVCAR-3)
IgG
HOSE
TOV-21G
SKOV-3
OVCAR-3
FU-OV-1
URI
PP1γ
B
HOSE
TOV-21G
SKOV-3
OVCAR-3
FU-OV-1
P-URI S371
URI
Tubulin
C
siRNA: Control/control
URI/control
PP1γ/control
URI/PP1γ
DAPI, Phalloidin, TUNEL
Fold change cell count
Fold change anaphase
Fold change TUNEL+cells
Control
URI
PP1
URI/PP1
D
siRNA:
Control/control
URI/control
PP1γ/control
URI/PP1γ
URI
PP1γ
P-S6K T389
S6K
P-BAD S136
BAD
PARP
Tubulin
E
PP1γ-IP
WCE (TOV-21G)
IgG
Control
IgG
HA-URI-WT
IgG
HA-URI-S371A
HA
URI
PP1γ
F
% serum:
2.5
5
10
Control
HA-URI-WT
HA-URI-S371A
2.5 % serum
5 % serum
%colonies relative to 10%serum
G
% serum:
2.5
5
10
Control
HA-URI-WT
HA-URI-S371A
HA
URI
PP1γ
P-S6K1 T389
S6K1
P-BAD S136
BAD
Tubulin
H
2.5 % serum
5 % serum
Fold change TUNEL+ cells to 10%serum
Control
HA-URI-WT
HA-URI-S371A
I
Xenograft
TOV-21G
Tumor volume (mm3)
Days
Control
HA-URI-WT
HA-URI-S371A
p=0.004

endogenous PP1γ than with HA-URI(wt) (Figure 4E). In clonogenic assays performed under various serum concentrations, the HA-URI(S371A)–producing pool grew significantly more colonies than the corresponding HA-URI(wt) –expressing pool or the vector control pool under low serum concentrations (Figure 4F). This difference was most evident at 5% or 2.5% serum concentrations (Figure 4F), indicating that conditions promoting constitutive URI-PP1γ complex formation confer a cell survival advantage. Consistent with these results, the phosphorylation status of S6K1 and BAD remained high in HA-URI(wt) or (S317A)–producing pools even under low serum concentrations (Figure 4G) and we observed less apoptotic cells under the same conditions (Figure 4H). Furthermore, in clonogenic assays, we also observed that *URI*-amplified OVCAR-3 and FU-OV-1 cells grew more efficiently under serum-limiting conditions than any of the non-*URI*-amplified SKOV-3, TOV-21G, and HOSE cells (Figure S4D). In agreement with the proposed molecular mechanism, in *URI*-amplified cells, phosphorylation of S6K1 was maintained under low serum concentrations, whereas in non-*URI*-amplified cells, phosphorylation of S6K1 was diminished (Figure S4D). Finally, by injecting TOV-21G cell pools expressing either HA-URI(wt) or HA-URI(S371A) into nude mice, we demonstrate accelerated tumor growth of TOV-21G cell pools producing the URI phosphosite mutant protein (Figure 4I). Collectively, these data suggest that URI acts as an ovarian cancer oncogene by increasing the threshold at which a cell initiates apoptosis in response to stressors such as low growth factor concentrations through constitutively inhibiting PP1γ and thereby allowing deregulated S6K1 survival signaling.

URI-Amplification and Overexpression Promotes Ovarian Cancer Cell Survival in an S6K1-Dependent Manner

As shown above, depletion of URI in ovarian cancer cells with *URI* amplification such as FU-OV-1 or OVCAR-3 causes dephosphorylation of S6K1 and BAD at Thr-389 and Ser-136, respectively. Similar effects on S6K1 phosphorylation were observed in other *URI* amplified cancer cell lines of nonovarian origin (Figure S5A). Depletion of URI in nonamplified ovarian cells did not cause significant dephosphorylation of S6K1 or BAD at the respective sites (Figure 5A). Nonamplified ovarian cancer cells were also more resistant to apoptosis in response to URI depletion (data not shown). Importantly, S6K1 was essential for efficient colony formation (Figure 5B) and cell survival (Figure 5C) for both (non-URI-amplified) TOV-21G and (*URI*-amplified) FU-OV-1 cells, consistent with a principal requirement for S6K1 for cell proliferation.

To directly test whether negative feedback inhibition of the S6K1-BAD survival axis is disabled in *URI*-amplified ovarian cancer cells, we depleted URI alone or in combination with overexpression of myc-tagged S6K1 in FU-OV-1 and scored for cell death. As expected, depletion of URI in these cells induced substantial cell death (Figure 5D). Importantly, cell death in this case was partially rescued by overexpression of myc-S6K1 (Figure 5D), suggesting that cell death observed in URI-depleted FU-OV-1 cells is caused, at least in part, by lower levels of S6K1 survival signaling. We also observed some cell death upon overexpression of myc-S6K1 (Figure 5D). This is likely due to S6K1-driven disruption of URI-PP1γ complexes, because in these cells little URI coimmunoprecipitated with PP1γ compared to control (Figure 5E), indicating that release of PP1γ had occurred. In accordance with this interpretation, myc-S6K1-overexpressing cells displayed reduced levels of BAD phosphorylation at Ser-136. In addition, myc-S6K1 overexpression counterbalanced dephosphorylation of BAD at Ser-136 caused by URI depletion (Figure 5F).

Next we examined whether this functional relationship between URI levels and phosphorylation status of S6K1 and BAD extend to human ovarian cancer tissue. Indeed, *URI* amplification and protein expression correlated significantly with the phosphorylation status of S6K1 and BAD in ovarian carcinoma tissues (Figure 5G). Similar correlations were found in other cancer types (Figure S5B). In fact, when analyzing gastric adenocarcinoma (because early ovarian lesions are extremely rare), we detected *URI* amplification already at the stage of noninvasive carcinoma in situ (5 of 5 cases). In this context, amplification and URI overexpression in glands of gastric carcinoma in situ matched with an increase in S6K1 phosphorylation and proliferation, whereas PP1γ expression did not change between normal glands and carcinoma in situ (Figure S5C). Combined, these results support a potential role for deregulated URI expression in promoting increased S6K1-BAD survival signaling already at an early stage in at least a subset of human cancers.

Figure 4. URI-Amplifed Ovarian Cancer Cells Are Characterized by Increased Abundance of URI-PP1γ Complexes

(A) Immunoprecipitation of equal amounts of PP1γ from the indicated ovarian cell lines and immunoblotting for URI and PP1γ. A whole cell extract (WCE) of OVCAR-3 cells was directly processed for immunoblotting and served as migration control for indicated proteins.

(B) Immunoblotting for URI and phospho-URI S371 on indicated cell lines.

(C) Knockdown of URI, PP1γ, and URI + PP1γ in FU-OV-1 cells by siRNA, TUNEL staining, anaphases, and cell count with quantification of three independent experiments in triplicate (*$p < 0.05$ and **$p < 0.01$, Student's t test). Bars represent 15 μM.

(D) Corresponding immunoblot analysis against the total proteins and phosphosites as indicated.

(E) PP1γ-immunoprecipitation blotted for indicated proteins on cells with retroviral-mediated overexpression of HA-tagged wild-type URI and a S371A mutant in TOV-21G cells. WCEs of TOV-21G cells were directly processed for immunoblotting and served as migration control for indicated proteins.

(F) Clonogenic assay with different serum concentrations and quantification in TOV-21G cells of three independent experiments in triplicate (*$p < 0.05$ and **$p < 0.01$, Student's t test).

(G) Immunoblotting analysis against the total proteins and phosphosites as indicated.

(H) TUNEL of TOV-21G cells cultured under different serum concentrations of three independent experiments in triplicate (*$p < 0.05$ and **$p < 0.01$, Student's t test).

(I) Tumor growth of TOV-21G cells with retroviral-mediated overexpression of HA-tagged wild-type URI and a S371A mutant in nude mice over time of ten mice per group (p value, Wilcoxon rank).

All error bars in the entire figure represent ± SD. See also Figure S4.

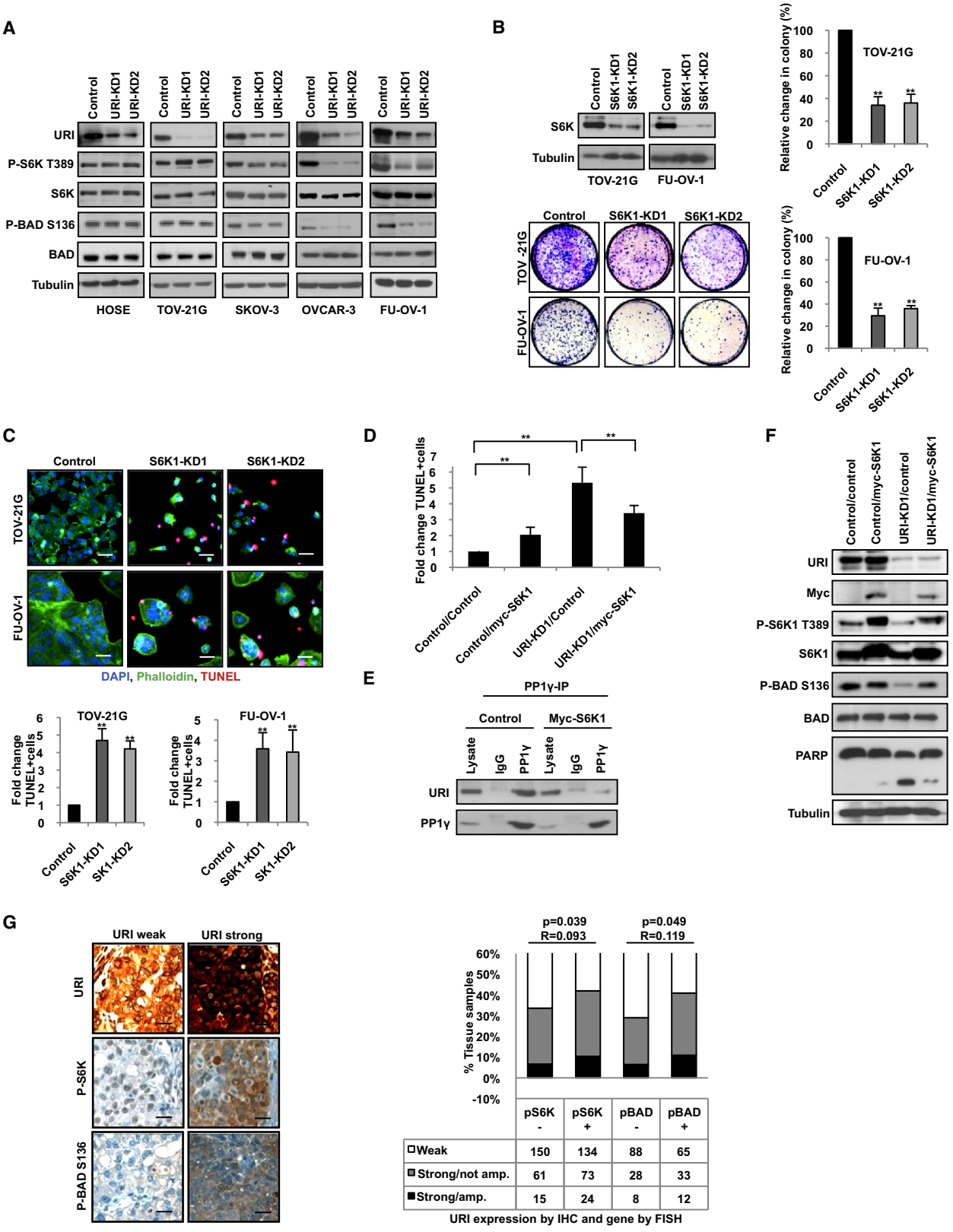

Figure 5. URI Maintains S6K1-Survival Signaling in Overexpressed Ovarian Cancer Cells

(A) Immunoblot analysis of HOSE, TOV-21G, SKOV-3, OVCAR-3, and FU-OV-1 ovarian cell lines after URI knockdown against the proteins and phosphosites indicated.

URI-Amplification and Overexpression Correlates with Resistance of Ovarian Cancer Cells to Rapamycin

Our data suggest that *URI* amplification affects PI3K-mTOR signaling in ovarian cancer cells downstream at the level of S6K1. Therefore, we asked next whether *URI*-amplified and non-*URI*-amplified ovarian cancer cells display differential sensitivity toward the mTOR inhibitor rapamycin in a colony formation assay. Indeed, already low concentrations of rapamycin inhibited colony formation of the non-*URI*-amplified cell lines HOSE, TOV-21G, and SKOV-3, whereas the *URI*-amplified cell lines OVCAR-3 and FU-OV-1 were significantly less sensitive to rapamycin (Figure 6A). Immunoblotting confirmed that in the former set of non-*URI*-amplified cell lines, S6K1 phosphorylation was inhibited in a dose-dependent manner, whereas in the latter set of *URI*-amplified cell lines, S6K1 phosphorylation persisted in the presence of rapamycin (Figure 6A). Importantly, phosphorylation of 4EBP1, another known downstream effector of mTOR, was inhibited to similar extend in all cell lines (Figure 6A), further supporting the notion that the URI-PP1γ axis targets selectively the S6K1 signaling branch. The importance of maintaining active S6K1 for efficient colony formation in *URI*-amplified cells is illustrated by the fact that OVCAR-3 and FU-OV-1 like non-*URI*-amplified cell lines display significantly reduced colony formation capacity following shRNA-mediated knockdown of S6K1 (Figure 6B). Immunoblotting confirmed efficient down-regulation of S6K1 in each of these cell lines under investigation (Figure 6B). Therefore, similar to what is observed under conditions of serum limitations, *URI* amplification mediates increased resistance to rapamycin.

URI Overexpression in Ovarian Cancer Cells Mediates Resistance to Cisplatin

The 19q12 amplicon was recently identified in a genomewide screen and was shown to correlate with resistance against platinum-based chemotherapy in ovarian cancer (Etemadmoghadam et al., 2009). In addition, *URI* amplification correlates with the failure of ovarian cancer cells to respond to platin-based chemotherapy (see Figure 1G). In light of its role in suppressing PP1γ-mediated negative feedback, we asked whether overexpression of URI contributes to resistance against cisplatin. Clonogenic assays revealed that overexpression of either HA-URI (wt) or HA-URI(S371A) mutant in otherwise cisplatin-sensitive TOV-21G cells promoted cisplatin-resistance in a PP1γ-dependent manner (Figure 7A). Interestingly, treatment of TOV-21G cells for 4–7 hr with cisplatin induced both S6K1 and BAD phosphorylation (Figure 7B). At 14 hr, phosphorylation of S6K1 and BAD was diminished again and poly(ADP-ribose) polymerase (PARP)-cleavage, as an indicator of cell death, was detectable (Figure 7B). TOV-21G cell pools stably expressing HA-URI(wt) or HA-URI(S371A) enhanced the effect of cisplatin on the phosphorylation of S6K1 and BAD, consistent with the notion that URI had entrapped and inhibited PP1γ resulting in increased S6K1 survival signaling. Indeed, when TOV-21G cells were depleted for S6K1 and treated with cisplatin, we observed further reduction in cell viability compared to cisplatin treatment alone (Figure 7C). Similar effects were observed for OVCAR-3 cells (Figure 7C). In FU-OV-1 cells, we did not observe such a synergism between S6K1 depletion and cisplatin (Figure 7C). This finding implies that ovarian cancer cells display, in the context of cisplatin treatment, different degrees of dependencies for S6K1 survival signaling. Depletion of URI sensitized selectively *URI*-amplified OVCAR-3 but not the non-*URI*-amplified TOV-21G cells to cisplatin (Figure 7D). This is consistent with the observation that, in *URI*-amplified OVCAR-3 cells, S6K1 activity is dependent on URI expression (Figure 5A). As one would expect, URI depletion did not further reduce cell viability of cisplatin-treated FU-OV-1 cells (Figure 7C). These data imply that in ovarian cancer cells *URI* amplification contributes to cisplatin resistance, at least in part, by modulating S6K1 signaling.

DISCUSSION

Here we report that a subset of both established ovarian cancer cell lines and advanced human ovarian cancers are characterized by amplification and overexpression of *URI*, a gene whose product acts as an inhibitor of PP1γ and thus PP1γ-mediated inactivation of S6K1 survival signaling. Only ovarian cancer cell lines that feature increased *URI* gene copy number at 19q12 experience a survival defect and decreased S6K1 activity after deprivation of URI by RNAi, effects that were overridden when the same cells were also depleted for PP1γ. Such cell lines, when deprived of URI, were also severely compromised for de novo tumorigenesis in nude mice. Moreover, conditional depletion of URI after tumor establishment also blocked subsequent tumor growth in vivo. Conversely, in ovarian cancer cell lines lacking *URI* amplification, overexpression of URI caused sustained S6K1 activity and BAD phosphorylation under conditions of growth-factor limitations, enhanced cell proliferation and tumor growth in vivo. In addition, these otherwise cisplatin-sensitive ovarian cancer cells converted upon overexpression of URI to cisplatin-resistant cells, consistent with the observed positive correlation between resistance of ovarian cancer cells to cisplatin and amplification of *URI*. Taken together, these findings strongly support the conclusion that *URI* functions as an ''addicting'' oncogene that supports uncontrolled cell

(B) Immunoblot analysis of S6K1 knockdown in TOV-21G and FU-OV-1 cells with two different shRNAs and clonogenic assay of these cells with the respective quantification.
(C) TUNEL staining and quantification of TOV-21G and FU-OV-1 cells after S6K1 knockdown with two different shRNAs. Bars represent 20 μM.
(D) TUNEL staining and quantification of FU-OV-1 cells with knockdown (KD1) of URI and overexpression of myc-tagged S6K1.
(E) PP1γ-immunoprecipitation blotted for indicated proteins on cells transfected with control and myc-tagged S6K1 overexpression in FU-OV-1 cells.
(F) Corresponding immunoblot analysis against the proteins and phosphosites indicated.
(G) Correlations of URI, P-S6K1 (T421/S424) (pS6K), and P-BAD S136 on ovarian carcinoma TMA (R = correlation coefficient, p value, Kendall beta-tau). Staining pattern exemplified on tumors with weak or strong URI expression. Bars represent 20 μm. Differences in number of cases among immunohistochemical markers were due to tissue damage (either tissue loss or inadequate tumor tissue).
All error bars in the entire figure represent ± SD of three independent experiments in triplicate (*$p < 0.05$ and **$p < 0.01$, Student's t test). See also Figure S5.

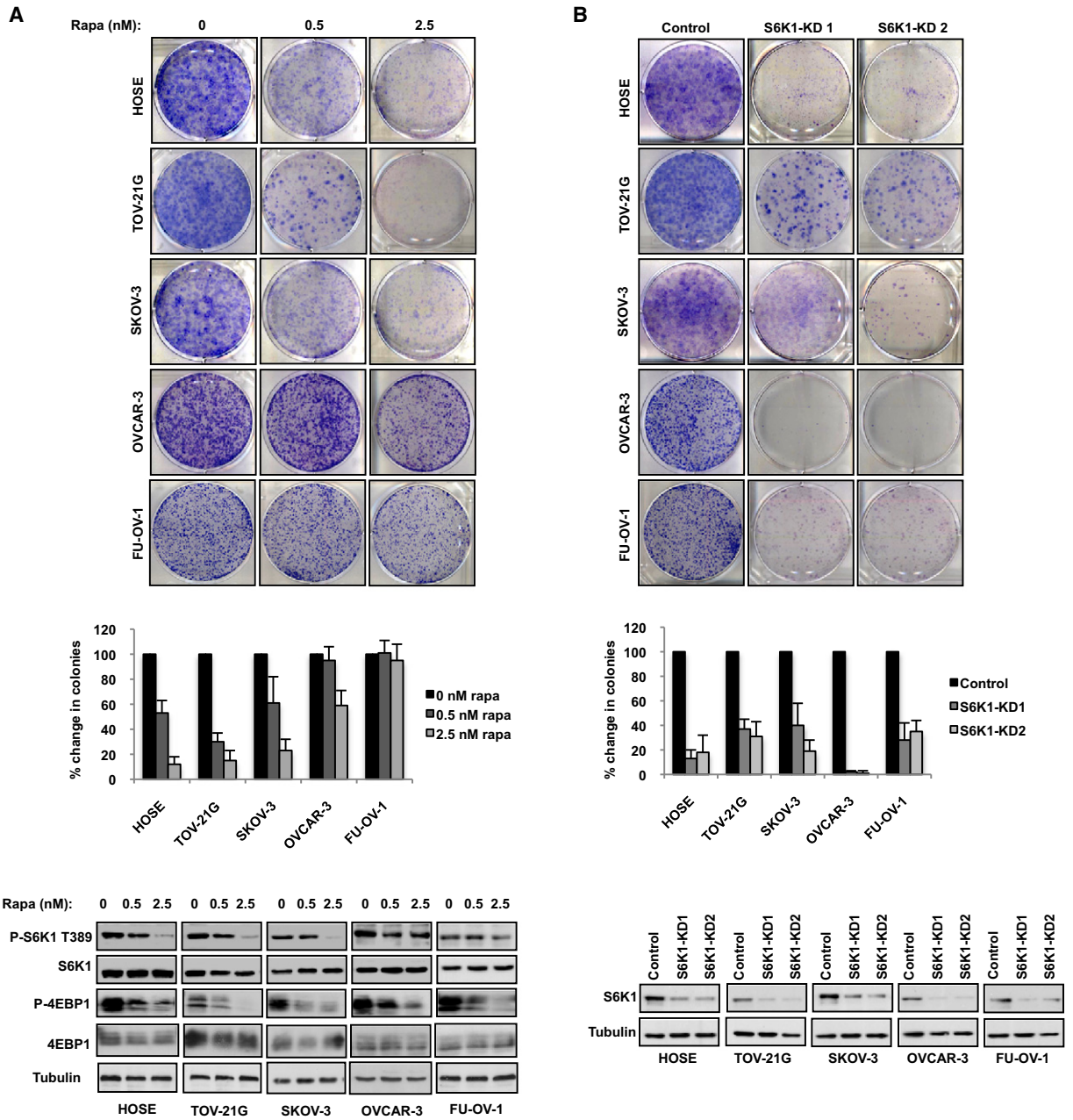

Figure 6. *URI*-Amplified Cells Are More Resistant to mTOR Inhibition by Rapamycin

(A) Clonogenic assays of the primary human HOSE, TOV-21G, SKOV-13, OVCAR-3, and FU-OV-1 cells with the indicated rapamycin concentrations and corresponding quantification. Corresponding immunoblotting for indicated proteins at various serum concentrations.

(B) Clonogenic assays of the indicated cell lines with S6K1-knockdown mediated by two different short-hairpins and corresponding quantification. Corresponding immunoblotting for knock-down validation.

All error bars in the entire figure represent ± SD of three independent experiments in triplicate.

proliferation and contributes to chemotherapy resistance of certain ovarian cancer cells by disabling a PP1γ-mediated negative feedback pathway that normally acts to restrain S6K1 survival signaling. The fact that *URI* amplification is observed in several distinct cancer types implies that abrogation of this negative feedback pathway may represent a key mechanism of apoptosis evasion during tumor cell evolution.

The biological effect of the 19q12 amplicon has been traditionally linked to *CCNE1*, the gene encoding then positive cell cycle regulator cyclin E (Lin et al., 2000; Nakanishi et al., 2000; Schraml et al., 2003). Congruently, this locus has been found to correlate with increased cell proliferation and tumor growth. However, an early report on gastric adenocarcinoma reported that, in some cases, gene amplification at 19q12 was not associated with

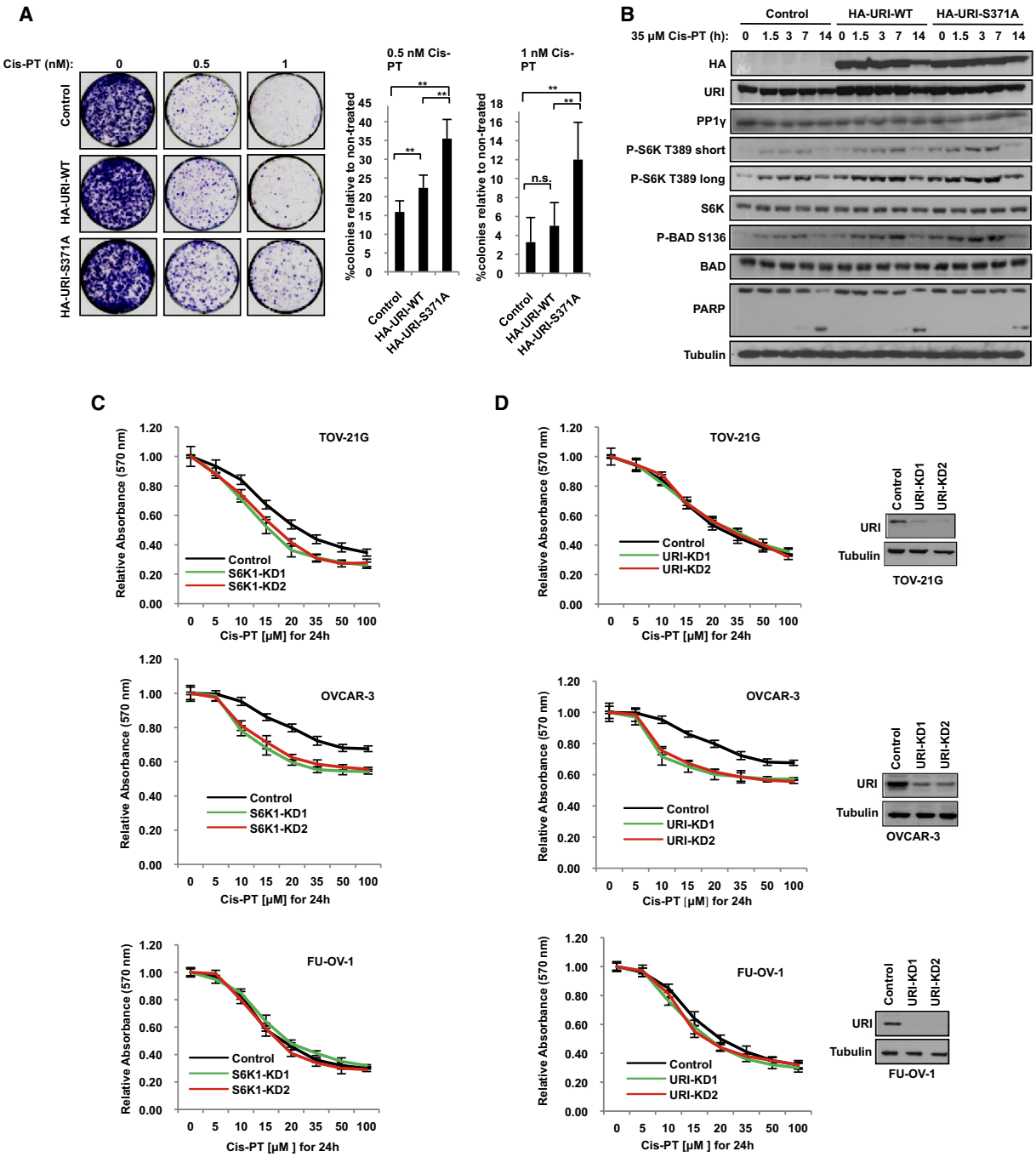

Figure 7. URI Overexpression in Ovarian Cancer Cells Mediates Resistance to Cisplatin

(A) Clonogenic assay and quantification of TOV21-G cells with vector control and an overexpression of HA-tagged wild-type URI and S371A mutant.

(B) Immunoblotting for proteins and phosphosites as indicated of a time-course experiment at 3.5% serum concentration in TOV-21G cells with vector control and an overexpression of HA-tagged wild-type URI and S371A mutant.

(C) MTT cell viability assay with control and knockdown of S6K1 in TOV-21G, OVCAR-3, and FU-OV-1 cells (for corresponding knockdown efficacy, see Figure 5B and Figure 6B).

(D) MTT cell viability assay with control and knockdown of URI in TOV-21G, OVCAR-3, and FU-OV-1 cells (left panels). Immunoblotting for URI in URI-knockdown TOV-21G, OVCAR-3, and FU-OV-1 cells (right panels).

All error bars in the entire figure represent ±SD of three independent experiments in triplicate (*$p < 0.05$ and **$p < 0.01$, Student's t test).

DNA copy number gain at *CCNE1*, concluding that other genes within this region may have important functions in tumor development (Leung et al., 2006). In this regard, a recent report suggested an association of amplification at 19q12 with chemotherapy resistance in ovarian cancer (Etemadmoghadam et al., 2009). Our results functionally link URI overexpression to

suppression of apoptosis and hence chemotherapy resistance. The anatomical proximity of *CCNE1* and *URI* at 19q12 may provide for many carcinomas a unique opportunity of a selective advantage through coamplification of key genes involved in promoting cell cycle (*CCNE1*) and cell survival (*URI*). This might also help to explain why 19q12-amplified carcinomas have such a poor prognosis among ovarian carcinomas. Although highest URI protein levels were observed in the context of gene amplification at chromosome 19q12, a substantial amount of ovarian carcinomas expressed also high levels of *URI* mRNA and protein in the absence of gene amplification, indicating that additional, yet to be elucidated mechanisms may contribute to URI overexpression and suppression of apoptosis.

At the root of apoptosis, evasion mediated by oncogenic activation of URI appears to be the previously described inhibitory interaction of URI with PP1γ at mitochondria (Djouder et al., 2007). According to the proposed model, acute growth factor and nutrient-dependent activation of S6K1 leads not only to phosphorylation of BAD at mitochondria but also to that of URI at Ser-371. The latter event causes disruption of URI-PP1γ complexes releasing PP1γ, which in turn, proceeds to dephosphorylate and inactivate S6K1 as part of a negative feedback system dedicated to dampen S6K1 survival signaling. Accordingly, for cancer cells to achieve increased S6K1 survival signaling output under stress conditions such as growth factor limitations, one or more aspects of this negative feedback system must be abrogated by oncogenic events. On the basis of the results shown here, we propose that *URI* amplification and overexpression inactivates the feedback pathway by notoriously entrapping PP1γ in inactive complexes. In this regard, we observed no increase in Ser-371 phosphorylation of URI in ovarian cancer cells featuring *URI* amplification. Consistent with this, also much more PP1γ was bound to URI in *URI*-amplified ovarian cancer cells. This may also help to explain why URI depletion caused cell death selectively in ovarian cancer cells with *URI* gene copy number alterations.

An increasing number of reports indicate a role for S6K1 in cell survival, at least in part by its ability to sequester BAD from mitochondria (Datta et al., 2002; Djouder et al., 2007; Harada et al., 2001; Nakamura et al., 2008; Strobel et al., 1998). Indeed, we and others found that damaging agents such as chemotherapeutics and UV-irradiation promote S6K1 activity as part of an adaptive survival response (Dhar and Basu, 2008; Hartman et al., 2010; Huang et al., 2002; Lei et al., 2009; Shi et al., 1995; Strobel et al., 1998; Wu et al., 2005). In the context of tumorigenesis, a recently performed synthetic-lethality screen brought to light that K-ras–transformed cancer cells depend on S6K1-survival signaling (Scholl et al., 2009). Our data further highlight the importance of S6K1 in cancer cell survival by linking its activity, at least in part, to the 19q12 amplicon in ovarian cancer cells.

S6K1 represents one of several downstream targets of mTOR, which has emerged as a critical effector in cell signaling pathways commonly deregulated in human cancers. This has led to the prediction that mTOR inhibitors may be useful as anticancer agents. Indeed, derivatives of one such molecule, rapamycin, are currently in clinical development. The finding of a disabled negative feedback in a subset of ovarian cancer cells characterized by *URI* amplification combined with the observation that also fractions of other human cancers feature an amplification of *URI*, point to a possible resistance of these cancers to rapamycin or its derivatives. In support of this view, rapamycin was indeed less efficient in inhibiting S6K1 activity and colony formation in ovarian cancer cells in which negative feedback inhibition was disrupted by *URI* amplification. Of note, in these cancer cells, rapamycin did inhibit phosphorylation of 4EBP1, another downstream target of mTOR (Figure 6A). Therefore, it is conceivable to propose that oncogenic activation of *URI* disrupts cell signaling downstream of mTOR by affecting selectively the S6K1 survival signaling branch of this central growth regulatory pathway.

Taken together, our results add an important molecular mechanism of intrinsic apoptosis evasion in cancer and functionally link the 19q12 amplicon to apoptosis resistance of ovarian cancer cells and to platinum-based chemotherapy. The fact that down-regulation of URI selectively affects the viability of those cells that feature amplification of *URI* implies that it has properties of an ''addicting'' oncogene and provides an opportunity for targeted therapeutic intervention. A small molecule that specifically disrupts URI-PP1γ complexes could dramatically lower the apoptotic threshold in *URI*-amplified cancer cells. Such a drug could prove to be successful for the treatment of carcinomas with a 19q12 amplicon in combination with conventional chemotherapy or oncogenic kinase inhibitors.

EXPERIMENTAL PROCEDURES

Clonogenic Assays, TUNEL and Cell Proliferation, and MTT

For clonogenic assays, cells of the respective cell line were seeded in 6-well plates (NUNC) and grown under the indicated conditions. In the case of TOV-21G and HOSE cells, 5000 cells/well were seeded and cultured for 8 days. SKOV-3 cells were seeded at 3500 cells/well, FU-OV-1 at 7500 cells/well, and OVCAR-3 at 12,000 cells/well, respectively, and were cultured for 16 days. Plates were fixed and stained using Giemsa's azur eosin methylene blue (MERCK), diluted 1:1 in 100% methanol. The number of colonies (defined as cell clusters consisting of at least 50 cells) was quantified by Analysis software (Olympus Biosystems). For quantification of apoptotic cells and cellular proliferation, cells were seeded in 96-well plates (Microclear black, Greiner) and grown for 3 days, fixed with 4% paraformaldehyde for 10 min, stained with TUNEL (In Situ Cell Death Detection Kit, TMR red, Roche Applied Science), and counterstained with Phalloidin (Alexa fluor 488, Invitrogen) and DAPI (SIGMA) according to manufacturer's protocols. Number of cells and anaphases detected by DAPI and apoptotic figures detected by TUNEL were counted in nine 20× fields per well. For cell viability MTT assay, cells were seeded at high density in a 96-well format (NUNC) and were treated for 24 hr with the indicated concentrations of cisplatin (SIGMA). MTT viability assay was performed as described elsewhere (Fanning et al., 1990). Details regarding cell culture and immunoblotting can be found in the Supplemental Experimental Procedures.

SNP-Array

Genomic DNA was extracted using a DNeasy kit (QIAGEN) from FU-OV-1 and OVCAR-3 cells and subsequently analyzed for copy variation of nonpolymorphic probes by Affymetrix SNP 6.0 arrays according to manufacturer's protocol. Absolute signal intensities normalized to corresponding set of HapMap references were displayed in the Smooth Signal Mode.

Human Tumor Samples

Tumor specimens and clinical data were obtained from two different cohorts, the Institute of Surgical Pathology and the local cancer registry at the University Hospital Zurich and Basel, with the approval of the institutional review boards and the local ethics committee of the Kanton Zurich, Switzerland. Informed consent was obtained from all subjects (reference numbers StV

12-2005, 27-2009, 29-2007, and KEK-ZH 2010-0093/0). Details on the characterization of the clinical data and different TMAs can be found in Supplemental Experimental Procedures.

Immunohistochemistry and FISH

For the detection of P-S6K1 (T421/S424), Ki-67, and P-BAD (S136), slides were analyzed with the Ventana Benchmark automated staining system (Ventana Medical Systems, Tucson, Arizona) using Ventana reagents for the entire procedure. For antigen retrieval, slides were heated with cell-conditioning solution for 1 hr (CC1; Tris-based buffer with slightly alkaline pH) using a standard protocol. Thereafter, slides were incubated with the primary antibodies at following concentrations: P-S6K1 (1:100), ki-67 (1:100), and P-BAD (1:100) for 1 hr. Detection was performed using the UView HRP system (Ventana Medical Systems, Tucson, Arizona). In the case of URI and PP1γ, slides were analyzed with the BondMax staining system (Vision BioSystems, acquired by Leica Microsystems). For antigen retrieval, slides were heated with cell-conditioning solution for 30 min (H1; Tris-based buffer with slightly alkaline pH). Then, slides were incubated with the primary antibodies at following concentrations: URI (1:500) and PP1γ 1:100 for 1 hr. Detection was carried out using the Bond Intense R Detection kit, according to the manufacturer's recommendations. Details on the scoring of staining pattern and FISH against *URI* can be found in Supplemental Experimental Procedures.

Xenograft Studies

All animal work was performed in accordance with the guidelines of the Institutional Animal Care and local veterinary office and ethics committee of the Kanton Zurich, Switzerland (reference number 199/2008) under approved protocols. To study primary tumorigenesis, TOV-21G cells harvested from culture were resuspended in PBS at a concentration of 2.5×10^6 cells/ml and were injected subcutaneously into female athymic nude mice. For OVCAR-3 cells, the corresponding procedure has been described elsewhere (Hamilton et al., 1983). We created a regulable Tet-Off OVCAR-3 cell line, which expresses a microRNA-based hairpin against URI (Open Biosystems V2HS_23227) after doxycycline withdrawal from the medium, as described elsewhere (Dickins et al., 2005). More specifically, we used two different clones, which were validated by western blot and colony formation assays (Figure S2D). Doxycycline (2 mg/ml) was administered in the drinking water before and after injection of the cells. It was withdrawn from the drinking water after tumors had formed. Primary tumor volume was measured every 3 days.

Statistical Analysis

The Kaplan-Meier method was used to estimate survival curves for human patients and log-rank was used to evaluate statistical differences. Kendall's tau-beta was used for correlating ordinal expression variables on TMAs with each other. A two-sided independent Student's t test without equal variance assumption was performed to analyze the results of cell culture experiments. Wilcoxon rank test was used for evaluating differences within tumor growth of TOV-21G cells with and without overexpression of HA-tagged URI constructs.

ACCESSION NUMBERS

SNP-array data on FU-OV-1 and OVCAR-3 cells have been deposited in the Gene Expression Omnibus website with accession code GSE26301.

SUPPLEMENTAL INFORMATION

Supplemental Information includes five figures and Supplemental Experimental Procedures and can be found with this article online at doi:10.1016/j.ccr.2011.01.019.

ACKNOWLEDGMENTS

We thank all members of the laboratories for helpful discussions. We also thank Stefan Neuenschwander from the Functional Genomics Center Zurich, for the analysis of the SNP-array data, and T. Rudolph, S. Behnke, and M. Storz for skillful technical assistance. We thank the Tissue Tumor Bank of the University Hospital Zurich for providing tissues. J.P.T. is funded by the Gertrud-Hagmann-Stiftung für Malignomforschung arranged by the Swiss Group for Clinical Cancer Research, by a grant from the Swiss Cancer League (KLS–02014-02-2007), and by the Julius Müller Stiftung zur Unterstützung der Krebsforschung.

Received: May 19, 2010
Revised: November 9, 2010
Accepted: January 7, 2011
Published: March 14, 2011

REFERENCES

Bergmann, A. (2002). Survival signaling goes BAD. Dev. Cell *3*, 607–608.

Danial, N.N., Gramm, C.F., Scorrano, L., Zhang, C.Y., Krauss, S., Ranger, A.M., Datta, S.R., Greenberg, M.E., Licklider, L.J., Lowell, B.B., et al. (2003). BAD and glucokinase reside in a mitochondrial complex that integrates glycolysis and apoptosis. Nature *424*, 952–956.

Datta, S.R., Ranger, A.M., Lin, M.Z., Sturgill, J.F., Ma, Y.C., Cowan, C.W., Dikkes, P., Korsmeyer, S.J., and Greenberg, M.E. (2002). Survival factor-mediated BAD phosphorylation raises the mitochondrial threshold for apoptosis. Dev. Cell *3*, 631–643.

Dhar, R., and Basu, A. (2008). Constitutive activation of p70 S6 kinase is associated with intrinsic resistance to cisplatin. Int. J. Oncol. *32*, 1133–1137.

Dickins, R.A., Hemann, M.T., Zilfou, J.T., Simpson, D.R., Ibarra, I., Hannon, G.J., and Lowe, S.W. (2005). Probing tumor phenotypes using stable and regulated synthetic microRNA precursors. Nat. Genet. *37*, 1289–1295.

Djouder, N., Metzler, S.C., Schmidt, A., Wirbelauer, C., Gstaiger, M., Aebersold, R., Hess, D., and Krek, W. (2007). S6K1-mediated disassembly of mitochondrial URI/PP1gamma complexes activates a negative feedback program that counters S6K1 survival signaling. Mol. Cell *28*, 28–40.

Etemadmoghadam, D., deFazio, A., Beroukhim, R., Mermel, C., George, J., Getz, G., Tothill, R., Okamoto, A., Raeder, M.B., Harnett, P., et al. (2009). Integrated genome-wide DNA copy number and expression analysis identifies distinct mechanisms of primary chemoresistance in ovarian carcinomas. Clin. Cancer Res. *15*, 1417–1427.

Fanning, J., Biddle, W.C., Goldrosen, M., Crickard, K., Crickard, U., Piver, M.S., and Foon, K.A. (1990). Comparison of cisplatin and carboplatin cytotoxicity in human ovarian cancer cell lines using the MTT assay. Gynecol. Oncol. *39*, 119–122.

Gstaiger, M., Luke, B., Hess, D., Oakeley, E.J., Wirbelauer, C., Blondel, M., Vigneron, M., Peter, M., and Krek, W. (2003). Control of nutrient-sensitive transcription programs by the unconventional prefoldin URI. Science *302*, 1208–1212.

Hamilton, T.C., Young, R.C., McKoy, W.M., Grotzinger, K.R., Green, J.A., Chu, E.W., Whang-Peng, J., Rogan, A.M., Green, W.R., and Ozols, R.F. (1983). Characterization of a human ovarian carcinoma cell line (NIH:OVCAR-3) with androgen and estrogen receptors. Cancer Res. *43*, 5379–5389.

Hanahan, D., and Weinberg, R.A. (2000). The hallmarks of cancer. Cell *100*, 57–70.

Harada, H., Andersen, J.S., Mann, M., Terada, N., and Korsmeyer, S.J. (2001). p70S6 kinase signals cell survival as well as growth, inactivating the pro-apoptotic molecule BAD. Proc. Natl. Acad. Sci. USA *98*, 9666–9670.

Hartman, M.L., Esposito, J.M., Yeap, B.Y., and Sugarbaker, D.J. (2010). Combined treatment with cisplatin and sirolimus to enhance cell death in human mesothelioma. J. Thorac. Cardiovasc. Surg. *139*, 1233–1240.

Hu, J., Khanna, V., Jones, M.W., and Surti, U. (2003). Comparative study of primary and recurrent ovarian serous carcinomas: comparative genomic hybridization analysis with a potential application for prognosis. Gynecol. Oncol. *89*, 369–375.

Huang, C., Li, J., Ke, Q., Leonard, S.S., Jiang, B.H., Zhong, X.S., Costa, M., Castranova, V., and Shi, X. (2002). Ultraviolet-induced phosphorylation of p70(S6K) at Thr(389) and Thr(421)/Ser(424) involves hydrogen peroxide and mammalian target of rapamycin but not Akt and atypical protein kinase C. Cancer Res. *62*, 5689–5697.

Johnstone, R.W., Ruefli, A.A., and Lowe, S.W. (2002). Apoptosis: a link between cancer genetics and chemotherapy. Cell *108*, 153–164.

Klumpp, S., and Krieglstein, J. (2002). Serine/threonine protein phosphatases in apoptosis. Curr. Opin. Pharmacol. *2*, 458–462.

Lei, W., Jia, T., Su, Z., Wen, W., and Zhu, X. (2009). Combined effect of rapamycin and cisplatin on survival of Hep-2 cells in vitro. Oncol. Res. *18*, 73–81.

Leung, S.Y., Ho, C., Tu, I.P., Li, R., So, S., Chu, K.M., Yuen, S.T., and Chen, X. (2006). Comprehensive analysis of 19q12 amplicon in human gastric cancers. Mod. Pathol. *19*, 854–863.

Lin, L., Prescott, M.S., Zhu, Z., Singh, P., Chun, S.Y., Kuick, R.D., Hanash, S.M., Orringer, M.B., Glover, T.W., and Beer, D.G. (2000). Identification and characterization of a 19q12 amplicon in esophageal adenocarcinomas reveals cyclin E as the best candidate gene for this amplicon. Cancer Res. *60*, 7021–7027.

Nakamura, J.L., Garcia, E., and Pieper, R.O. (2008). S6K1 plays a key role in glial transformation. Cancer Res. *68*, 6516–6523.

Nakanishi, M., Sakakura, C., Fujita, Y., Yasuoka, R., Aragane, H., Koide, K., Hagiwara, A., Yamaguchi, T., Nakamura, Y., Abe, T., et al. (2000). Genomic alterations in primary gastric cancers analyzed by comparative genomic hybridization and clinicopathological factors. Hepatogastroenterology *47*, 658–662.

Scholl, C., Frohling, S., Dunn, I.F., Schinzel, A.C., Barbie, D.A., Kim, S.Y., Silver, S.J., Tamayo, P., Wadlow, R.C., Ramaswamy, S., et al. (2009). Synthetic lethal interaction between oncogenic KRAS dependency and STK33 suppression in human cancer cells. Cell *137*, 821–834.

Schraml, P., Bucher, C., Bissig, H., Nocito, A., Haas, P., Wilber, K., Seelig, S., Kononen, J., Mihatsch, M.J., Dirnhofer, S., and Sauter, G. (2003). Cyclin E overexpression and amplification in human tumours. J. Pathol. *200*, 375–382.

Shi, Y., Frankel, A., Radvanyi, L.G., Penn, L.Z., Miller, R.G., and Mills, G.B. (1995). Rapamycin enhances apoptosis and increases sensitivity to cisplatin in vitro. Cancer Res. *55*, 1982–1988.

Siegert, R., Leroux, M.R., Scheufler, C., Hartl, F.U., and Moarefi, I. (2000). Structure of the molecular chaperone prefoldin: unique interaction of multiple coiled coil tentacles with unfolded proteins. Cell *103*, 621–632.

Snijders, A.M., Nowee, M.E., Fridlyand, J., Piek, J.M., Dorsman, J.C., Jain, A.N., Pinkel, D., van Diest, P.J., Verheijen, R.H., and Albertson, D.G. (2003). Genome-wide-array-based comparative genomic hybridization reveals genetic homogeneity and frequent copy number increases encompassing CCNE1 in fallopian tube carcinoma. Oncogene *22*, 4281–4286.

Strobel, T., Tai, Y.T., Korsmeyer, S., and Cannistra, S.A. (1998). BAD partly reverses paclitaxel resistance in human ovarian cancer cells. Oncogene *17*, 2419–2427.

Wu, C., Wangpaichitr, M., Feun, L., Kuo, M.T., Robles, C., Lampidis, T., and Savaraj, N. (2005). Overcoming cisplatin resistance by mTOR inhibitor in lung cancer. Mol. Cancer *4*, 25.